Table IV. Electrolyte Dependence of the Coverage-Normalized Conductance of Mixed-Valent (III/II) Polymers

complex	electrolyte	anion diameter, Å	g/Γ
$[Os(v\text{-}bpy)_3]^{2+}$	TBAP	3.70	3.81×10^7
$[Os(v\text{-}bpy)_3]^{2+}$	$(TBA)BF_4$	4.35	2.59×10^7
$[Os(v\text{-}bpy)_3]^{2+}$	$(TBA)PF_6$	3.34	2.63×10^7
$[Fe(v\text{-}bpy)_2(CN)_2]$	TBAP	3.70	2.80×10^8
$[Fe(v\text{-}bpy)_2(CN)_2]$	(TMA)Ts	7.98	3.18×10^8

to explain conductances in these polymers.

Consistent with this theory is the observation that the conductance observed for the Co(II/I) couple is several orders of magnitude higher than that for the Co(II/III) couple for polymerized films of $[Co(v\text{-}terpy)_2]^{2+}$. These values follow the same trend as the apparent diffusion coefficients measured by chronoamperometry.[31] Also, the conductance for the $[Os(5\text{-}Cl\text{-}phen)_3]^{2+/3+}$ mixed-valent polymer film is higher than that observed for the $[Os(v\text{-}bpy)_3]^{2+/3+}$ film, while the coordination environments are very similar except for the much shorter electron-hopping distance for the $[Os(5\text{-}Cl\text{-}phen)_3]^{2+/3+}$ polymer film due to its polymerization mechanism. The intrinsic energy barrier to hopping is thus reduced for smaller hopping distances, leading to increased electron mobility.

One further possible explanation for the observed behavior of these polymer films is that mobile counterions (rather than electrons) from the external solution maintain the charge mobility. This mechanism is often referred to as a type of ionic conduction. A variety of different-sized anions with the same charge were used in the supporting electrolyte, since if ions were responsible for the conduction, the size of the ion would affect its magnitude. The use of the smallest anions (with their accompanying solvation spheres) should result in the largest conductances. However, as shown in Table IV, the size of the anion had relatively little effect on the conductances. In acetonitrile, with 0.1 M supporting electrolyte, the use of various anions whose diameters ranged from 3.34 to 4.35 Å did not cause a significant difference in the normalized conductances for the $[Os(v\text{-}bpy)_3]^{2+/3+}$ polymer film. Similarly, in DMF, even the very large toluenesulfonate anion did not reduce the conductance for the $[Fe(v\text{-}bpy)_2(CN)_2]^{0/+}$ polymer film. The tetraphenylborate anion would have been an interesting comparison due to its very large diameter; however, the anion oxidizes at potentials lower than those of the metal centers of interest. The indepencence of the conductance on the identity of the counteranion provides further evidence for charge transport via electrons. Furthermore, the large difference in redox conduction between the II/III and the I/0 mixed-valent states are difficult to reconcile if counterion mobility is limiting rather than electron transport, since the counterion diffusion rate would have to be significantly altered by a change in the polymer oxidation state.

The trends presented here demonstrate the influence of the atomic radius of the metal centers and the π-back-bonding ability of the ligands on conductance. This suggests that lowering the activation barrier between localized states (in this case each transition-metal complex) produces an increase in the conductance. Investigation of the appropriate copolymers may provide further insight into limiting factors in conduction.

Acknowledgment. Financial support by the Materials Science Center at Cornell University is gratefully acknowledged. H.C.H. acknowledges support by a fellowship from the Aerospace Corp. H.D.A. is a recipient of a Presidential Young Investigator Award (1984-1989) and a Sloan Fellowship (1987-1991).

Registry No. $[Os(v\text{-}bpy)_3]^{2+}$, 97056-94-5; $[Ru(v\text{-}bpy)_3]^{2+}$, 81315-14-2; $[Fe(v\text{-}phy)_3]^{2+}$, 81315-15-3; $[Co(v\text{-}terpy)_2]^{2+}$, 108270-57-1; $[Fe(v\text{-}bpy)_2(CN)_2]$, 119058-92-3; $[Os(v\text{-}bpy)_2(phen\text{-}dione)]^{2+}$, 124355-17-5; $[Os(v\text{-}bpy)_2(5\text{-}NH_2\text{-}phen)]^{2+}$, 124355-19-7; $[Os(5\text{-}Cl\text{-}phen)_3]^{2+}$, 124355-20-0.

(31) Guadalupe, A. R.; Usifer, D. A.; Potts, K. T.; Hurrell, H. C.; Mogstad, A.-L.; Abruña, H. D. *J. Am. Chem. Soc.* **1988**, *110*, 3462.

Contribution from the Departments of Chemistry, Louisiana State University, Baton Rouge, Louisiana 70803, and University of Louisville, Louisville, Kentucky 40506, and Control Research and Development, Upjohn Pharmaceuticals Limited, Tsukuba 300-42, Japan

Rotation of the Cyclopentadienyl Ligand in Bis(μ-carbonyl)bis(carbonylcyclopentadienyliron)(*Fe-Fe*) in the Solid State As Determined from Solid-State Deuterium NMR Spectroscopy

Maria I. Altbach,[1a] Yukio Hiyama,*[,1b] Richard J. Wittebort,*[,1c] and Leslie G. Butler*[,1d]

Received January 9, 1989

The motion of the cyclopentadienyl ring in $(\mu\text{-}CO)_2[FeCp^d(CO)]_2$ (Cp^d = ca. 70% deuteriated η^5-cyclopentadienyl) in the solid state has been studied from 100 to 300 K by solid-state deuterium NMR methods. The deuterium spin-lattice relaxation times show that the orientation of the cyclopentadienyl ligands, Cp, is averaged among the five sites of the ring with nearest-neighbor jump rates in the range 1.20 (24) $\times 10^7$ to 2.4 (5) $\times 10^{11}$ s^{-1}. The activation energy for the process is 12.5 (3) kJ/mol. The kinetic parameters obtained in this work are similar to the values for the reorientation of the cyclopentadienyl ligands in other organometallic compounds as determined with different techniques. The results of this work show that solid-state deuterium NMR spectroscopy uniquely complements existing techniques for the study of the motional properties in organometallic systems.

Introduction

In the last decade, deuterium NMR spectroscopy has become a very popular technique for the study of dynamic processes in the solid state.[2] This technique makes possible the investigation of different motional modes over a wide range of rates. Dynamic processes occurring with rates in the range 10^4-10^8 s^{-1} can be investigated by a line-shape analysis of the deuterium NMR spectrum of a powder. For motions on the order of and faster than 10^8 s^{-1}, the line shapes become independent of the exchange rate; an analysis of the partially relaxed spectra obtained from deuterium spin-lattice relaxation time (T_1) experiments is used to discriminate among the types and rates of motion. With the availability of computer programs capable of simulating both the

* To whom correspondence should be addressed.

(1) (a) Present address: Department of Chemistry, University of Arizona, Tucson, AZ 85721. (b) Present address: Upjohn Pharmaceutical Limited, 17th Floor, Green Tower Building 6-14-1, Nishi Shinjuka, Tokyo 160, Japan. (c) University of Louisville. (d) Louisiana State University.

(2) (a) Jelinski, L. W. *Annu. Rev. Matter. Sci.* **1985**, *15*, 359-77. (b) Torchia, D. A. *Annu. Rev. Biophys. Bioeng.* **1984**, *13*, 125-44. (c) Spiess, H. W. *Adv. Polym. Sci.* **1985**, *66*, 23-58.

0020-1669/90/1329-0741$02.50/0

line shapes of the fully relaxed spectra and of the partially relaxed spectra, as obtained from a T_1 experiment, solid-state deuterium NMR spectroscopy has developed into an excellent probe for the study of the motional modes and rates in various systems such as polymers, proteins, and lipids, as well as small organic molecules.[3] The selective incorporation of the inexpensive deuterium isotope so as to extract dynamic information at specific sites of the molecule makes this technique even more attractive. Nevertheless, despite these advantages, to the best of our knowledge there are no reported applications of this technique to organometallic compounds.

To test the applicability of solid-state deuterium NMR spectroscopy to study the motions of organometallic species, we decided to investigate a simple system: the cyclopentadienyl ligand. The rotation of cyclopentadienyl ligands in the solid state has been discussed widely in the literature. Most organometallic compounds possessing an η^5-cyclopentadienyl ligand (Cp) show unusual thermal parameters for the carbon atoms in the ring in the X-ray crystal structures.[4] The motional properties of cyclopentadienyl units in the solid state have been measured by techniques such as Raman spectroscopy,[5] quasi-elastic neutron scattering,[6] and proton NMR spin–lattice relaxation times.[7] From these studies it is known that the Cp ring rotates in the solid state about its C_5 axis of rotation with rates as fast as 10^{11} s^{-1} and that the relatively small rotational barriers are in the range 2–16 kJ/mol.

In the present work we are applying solid-state deuterium NMR techniques to determine the rates and the activation energy of the reorientation of the cyclopentadienyl rings in $(\mu\text{-CO})_2[\text{FeCp}^d(\text{CO})]_2$ (Cp^d = ca. 70% deuteriated η^5-cyclopentadienyl)

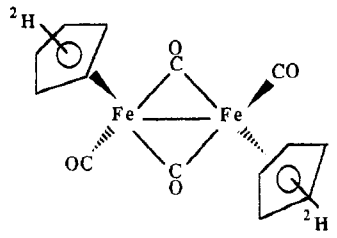

in the temperature range 100–300 K. A good agreement between the experimental and simulated data is obtained when the ring reorientation is interpreted by a model in which the ring is executing nearest-neighbor jumps about the C_5 axis of rotation (see I). The activation energy is 12.5 (3) kJ/mol, which is in the expected range for the reorientation of the Cp ring, according to the above-mentioned techniques applied to similar metal complexes. The preexponential factor obtained from the Arrhenius plot is 4.4 (8) × 10^{13} s^{-1}.

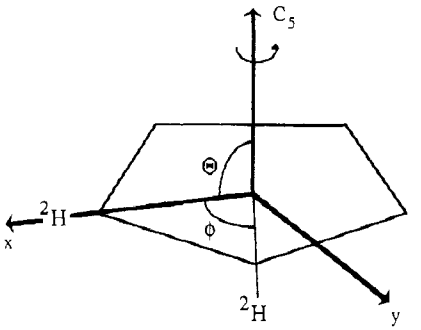

I

Experimental Section

Sample Preparation. $(\mu\text{-CO})_2[\text{FeCp}^d(\text{CO})]_2$ (Cp^d = ca. 70% deuteriated η^5-cyclopentadienyl) was prepared from deuteriated dicyclopentadiene and iron pentacarbonyl as described in the literature.[8] Crystals of $(\mu\text{-CO})_2[\text{FeCp}^d(\text{CO})]_2$ were obtained at room temperature so as to ensure the formation of the trans isomer.[9] The IR spectrum (KBr pellet) confirmed that the product obtained was *trans*-$(\mu\text{-CO})_2[\text{FeCp}^d(\text{CO})]_2$. The deuteriation of the cyclopentadienyl ring was carried out with literature procedures[10] by adding small portions of freshly distilled cyclopentadiene to boiling ^2H_2O. The two vapors were allowed to react by refluxing the vapor mixture for 5 min through a 35 × 350 mm column of neutral α-Al_2O_3 at 350 °C. At the end of the 5 min, the deuteriated cyclopentadiene was collected by distillation. This procedure was done twice. An unidentified impurity, detected by solution ^1H and ^2H NMR spectroscopy, codistilled with the cyclopentadiene. It was important not to reflux for more than 5 min; otherwise the formation of this impurity was favored. In order to purify the product of this low boiling point impurity, the deuteriated cyclopentadiene was allowed to dimerize and was then purified by fractional distillation. Once freed of the impurity, the deuteriated dicyclopentadiene was cracked, and the pure freshly distilled cyclopentadiene was left at room temperature for 1 week to ensure its quantitative conversion to the deuteriated dimer. The extent of deuteriation was determined from the ^1H NMR spectrum by comparing the ratio of intensities of the proton signal for the protiated and deuteriated cyclopentadiene relative to the intensity of the proton signal of a known quantity of $CHCl_3$ contained in a capillary tube concentric with the NMR tube.

Solid-State Deuterium NMR Spectroscopy. Solid-state deuterium NMR spectra were acquired at 30.7 MHz on a Bruker MSL200 solid-state NMR spectrometer provided with a temperature control unit that uses a copper–constantan thermocouple. In order to calibrate the variable-temperature unit, the resistance of a Lakeshore Cryotronics calibrated platinum resistor (calibration traceable to an NBS standard), placed inside the coil volume of an empty probe and installed in the magnet, was measured and compared to a calibration plot of resistance versus temperature;[11] this procedure was repeated for the six temperatures in the range 178–300 K. On the basis of this comparison, the copper–constantan thermocouple is accurate to within ±2 K. Care should be exercised in the low-temperature experiments to prevent freezing the O-ring seals about the bore tube of the superconducting magnet; a vacuum leak could quickly lead to loss of the magnetic field. With the nominal insulation about the Bruker wide-bore probe, the manufacturer's recommended low-temperature limit is 153 K. For a brief time, on the order of 6 h, data at 100 K were collected for the T_1 and T_2 anisotropy experiments.

The quadrupole echo pulse sequence used is as follows: $(90_{x,-x}\text{-}t_1\text{-}90_{y}\text{-}t_2\text{-}\text{acq}_{x,-x})$.[12] The 90° pulse length was 2.5 μs. The delay between 90° pulses, t_1, was 30 μs. Echo acquisition started after a delay, t_2 = 31 μs, after the second 90° pulse. A two-step phase-cycling routine, where the phase of the first 90° pulse and the receiver phase are alternated

(3) (a) Jelinski, L. W.; Dumais, J. J.; Engel, A. K. *Macromolecules* **1983**, *16*, 492–6. (b) Kinsey, R. A.; Kintanar, A.; Oldfield, E. *J. Biol. Chem.* **1981**, *256*, 9028–36. (c) Davis, J. H. *Biochim. Biophys. Acta* **1983**, *737*, 117–71. (d) Batchelder, L. S.; Niu, C. H.; Torchia, D. A. *J. Am. Chem. Soc.* **1983**, *105*, 2228–31. (e) Sarkar, S. K.; Young, P. E.; Torchia, D. A. *J. Am. Chem. Soc.* **1986**, *108*, 6459–64. (f) Gall, C. M.; DiVerdi, J. A.; Opella, S. J. *J. Am. Chem. Soc.* **1981**, *103*, 5039–43. (g) Beshah, K.; Olejniczak, E. T.; Griffin, R. G. *J. Chem. Phys.* **1987**, *86*, 4730–6. (h) Woehler, S. E.; Wittebort, R. J.; Oh, S. M.; Hendrickson, D. N.; Inniss, D.; Strouse, C. E. *J. Am. Chem. Soc.* **1986**, *108*, 2938–46. (i) Hiyama, Y.; Silverton, J. V.; Torchia, D. A.; Gerig, J. T.; Hammond, S. J. *J. Am. Chem. Soc.* **1986**, *108*, 2715–23.

(4) (a) Bryan, R. F.; Greene, P. T. *J. Chem. Soc. A* **1970**, 3064–8. (b) Mitschler, A.; Rees, B.; Lehmann, M. S. *J. Am. Chem. Soc.* **1978**, *100*, 3390–7. (c) Fitzpatrick, P. J.; Le Page, Y.; Sedman, J.; Butler, I. S. *Inorg. Chem.* **1981**, *20*, 2852–61. (d) Berndt, A. F.; Marsh, R. E. *Acta Crystallogr.* **1963**, *16*, 118–23. (e) Adams, R. D.; Collins, D. M.; Cotton, F. A. *Inorg. Chem.* **1974**, *13*, 1086–90. (f) Bryan, R. F.; Greene, P. T.; Newlands, M. J.; Field, D. S. *J. Chem. Soc. A* **1970**, 3068–74. (g) Fitzpatrick, P. J.; Le Page, Y.; Butler, I. S. *Acta Crystallogr., Sect. B* **1981**, *37*, 1052–8.

(5) Chhor, K.; Lucazeau, G. *Inorg. Chem.* **1984**, *23*, 462–8 and references therein.

(6) Lucazeau, G.; Chhor, K.; Sourisseau, C.; Dianoux, A. J. *Chem. Phys.* **1983**, *76*, 307–14.

(7) (a) Gilson, D. R. F.; Gomez, G.; Butler, I. S.; Fitzpatrick, P. J. *Can. J. Chem.* **1983**, *61*, 737–42. (b) Gilson, D. R. F.; Gomez, G. *J. Organomet. Chem.* **1982**, *240*, 41–7. (c) Campbell, A. J.; Fyfe, C. A.; Harold-Smith, D.; Jeffrey, K. R. *Mol. Cryst. Liq. Cryst.* **1976**, *36*, 1–23. (d) McGarvey, B. R.; Nagy, S. *Inorg. Chem.* **1987**, *26*, 4198–203.

(8) King, R. B. *Organometallic Synthesis*; Academic Press: New York, 1965; Vol. I, pp 114–5.

(9) *cis*-$(\mu\text{-CO})_2[\text{FeCp(CO)}]_2$ is formed when crystallization is carried out at low temperatures.[4f]

(10) Grimme, W.; von Eggers Doering, W. *Chem. Ber.* **1973**, *106*, 1765–80.

(11) Brandt, B. L.; Rubin, L. G.; Sample, H. H. *Rev. Sci. Instrum.* **1988**, *59*, 642–44.

(12) (a) Soloman, I. *Phys. Rev.* **1958**, *110*, 61–5. (b) Boden, N.; Levine, Y. K. *J. Magn. Reson.* **1978**, *30*, 327–42.

between 0 and 180°, was used in order to cancel the effects of probe ringing.[13] T_2 anisotropy measurements at 100 K were obtained by varying t_1 and t_2 in the quadrupole echo pulse sequence; the t_1 values used were 30, 60, 120, and 240 μs, and $t_2 = (t_1 + 1)$ μs. Spin–lattice relaxation times were measured by the inversion–recovery technique by applying a (180°–τ–) sequence prior to the quadrupole echo pulse sequence, where τ is a variable delay period. A total of 250 scans were averaged at each temperature. Two points at the beginning of the free induction decay (FID) data array were removed by left-shift of the data array so that the maximum intensity of the echo occurred at the first point in the data array, and a line-broadening factor of 1500 Hz was used in exponential multiplication to improve the signal-to-noise ratio of the spectrum. The delay between scans was adjusted to about 6 times the T_1 at the 90° orientation (vide infra) at each temperature to ensure that 99% of the magnetization was recovered before each scan. Typically, 12 variable delays, τ, were used for each T_1 experiment; 11 delays were used for 100-K experiments. The T_1 values at the 90° orientation, $T_1(90°)$, and at the 0° orientation, $T_1(0°)$ were calculated by fitting the spectral intensity at the corresponding frequency, $I(\tau)$, to the equation

$$I(\tau) = I_0\left[1 - 2A\exp\left(\frac{-\tau}{T_1}\right)\right] \quad (1)$$

where the three parameters T_1, I_0, and A were fitted by the Bruker program SIMFIT, which uses a Simplex routine.

Deuterium Line-Shape Simulations and T_1 Calculations. Simulations were performed on Micro VAX II and VAXstation 3500 computers using the powder pattern simulation program SPOWDER.[14] The input data set used by the program included the positions of the five sites among which the orientation of eq_{zz} is averaged, a matrix containing the jump rates between sites, the equilibrium probability of each site, the list of variable delays used in the T_1 experiment, the minimum number of orientations between the average eq_{zz} vector and the applied magnetic field necessary to simulate a smooth powder pattern, and the static quadrupole coupling constant. The program also takes into account the effect of finite pulse widths, a factor that tends to reduce the intensity of the shoulders of the experimental deuterium powder pattern.[15] For the model under study, the positions of the five sites are defined by polar angles (Θ and $(\tau - \phi)$, as shown in I, for each of the five $C-^2H$ bonds of the ring. The equilibrium probability for each of the five sites was set to 0.2. Smooth simulated powder patterns were obtained with a combination of 120 orientations of eq_{zz} with respect to the magnetic field and a line-broadening factor of 1500 Hz. The value of the quadrupole coupling constant was taken as 198 kHz (vide infra). The jump rate between nonneighboring sites (a C_5^2 rotation) was set to zero, and the jump rate, k, between neighboring sites (a C_5 rotation) was the sole remaining variable; an initial estimate of the rate was obtained from the theoretical curves, $T_1(0°)$ and $T_1(90°)$ versus log k, and the rate was varied until a good match between the simulated and experimental sets of powder patterns was obtained. The total computing time for the 12 partially relaxed spectra in the T_1 experiment is about 13 h on a Micro VAX II or 4 h on a VAXstation 3500.

Theory

A brief overview of solid-state deuterium NMR spectroscopy is presented here. In solid-state deuterium NMR spectroscopy, the spectrum is dominated by the quadrupolar interaction.[16] For aliphatic deuterons, the quadrupolar interaction arises mainly from the electrostatic coupling between the deuterium nuclear quadrupole moment, Q, and the electric field gradient along the $C-^2H$ bond.[17a,b] The characteristics of this interaction are reflected in the NMR experiment in two measurable parameters, the deuterium quadrupole coupling constant, $e^2q_{zz}Q/h$, and the asymmetry parameter, η. The principal component of the traceless electric field gradient tensor in the principal axis system is labeled eq_{zz} and lies closely along the $C-^2H$ bond axis.[17] The asymmetry parameter is a measure of the difference in magnitude between the other two principal components of the electric field gradient tensor, eq_{yy} and eq_{xx}; thus η has values between 0 and 1. When $\eta = 0$, the electric field gradient tensor is axially symmetric, which is typically the case for $C-^2H$ bonds.[17]

The deuterium nucleus has a nuclear spin $I = 1$, so in a high magnetic field, there are two allowed transitions among the spin states: the $|-1\rangle \rightarrow |0\rangle$ and the $|0\rangle \rightarrow |+1\rangle$.[18a] In powdered samples the line shape for each spin-state transition is determined by the random distribution of the $C-^2H$ bond orientations with respect to the direction of the magnetic field. The total line shape is a sum of the two separate powder patterns, one for each allowed transition. A typical deuterium NMR powder pattern for a rigid $C-^2H$ bond with axial symmetry is shown in II. The peaks of

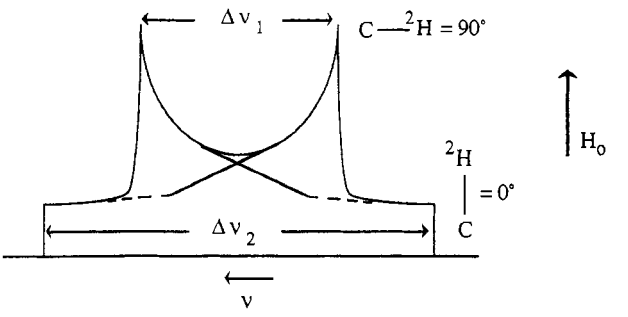

II

the line shape correspond to the contribution from $C-^2H$ bonds oriented at 90° (perpendicular) with respect to the direction of the magnetic field. The shoulders correspond to the 0° (parallel) orientation. For an asymmetry parameter of zero, the splitting between the peaks of the static powder pattern, $\Delta\nu_1$, is equal to $(3/4)e^2q_{zz}Q/h$, and the splitting between the shoulders, $\Delta\nu_2$, is twice $\Delta\nu_1$. For the deuterons in the Cp ring, $e^2q_{zz}Q/h$ is 198 (2) kHz, as measured for ferrocene-d_{10} from the experimental powder patterns at 113 K.[19]

Effect of Solid-State Dynamics on the Deuterium NMR Spectrum. When motions are present in the solid state, there are, with regard to the solid-state deuterium NMR spectrum, three exchange regimes in which the motional rate can fall. $C-^2H$ bonds that are moving with rates that are much less than the value of $e^2q_{zz}Q/h$ are in the slow-exchange regime. Rates that are on the time scale of the quadrupole interaction, $e^2q_{zz}Q/h \sim 10^5\ s^{-1}$, are in the intermediate-exchange regime. Finally, rates that are much larger than the value of $e^2q_{zz}Q/h$ are in the fast-exchange regime. For a Cp ring executing C_5 rotations, the slow-exchange regime is below $10^5\ s^{-1}$, and the fast-exchange regime starts at $10^8\ s^{-1}$. In the slow-exchange regime $C-^2H$ bonds are considered rigid and will display the type of spectrum described above, the static deuterium powder pattern.

As the motional rates increase past the slow-exchange limit, the spectral line shapes are greatly affected by the type and rate of motion.[14,16,18] This is illustrated in Figure 1, which shows the effect on the line shape as the rate of motion varies from the slow-exchange region to the fast-exchange region. Here the powder patterns are simulations of the fully relaxed spectra for the $C-^2H$ bonds in a Cp ring executing five-site nearest-neighbor jumps. It is important to note that as the rate approaches the intermediate-exchange regime, the effect of the rate on the line shape becomes more dramatic. In the intermediate-exchange region, there is also a loss of the spectral intensity, which is accentuated for certain spectral regions. Since the rates are comparable to the quadrupolar interaction in this region, the

(13) Fukushima, E.; Roeder, S. B. W. *Experimental Pulse NMR: A Nuts and Bolts Approach*; Addison-Wesley: Reading, MA, 1981; Chapter 5.
(14) Wittebort, R. J.; Olejniczak, E. T.; Griffin, R. G. *J. Chem. Phys.* **1987**, *86*, 5411–20.
(15) Bloom, M.; Davis, J. H.; Valic, M. I. *Can. J. Phys.* **1980**, *58*, 1510–7.
(16) Fyfe, C. A. *Solid State NMR for Chemists*; C. F. C. Press: Guelph, Ontario, Canada, 1983.
(17) (a) Huber, H. *J. Chem. Phys.* **1985**, *83*, 4591–8. (b) Altbach, M. I.; Hiyama, Y.; Gerson, D. J.; Butler, L. G. *J. Am. Chem. Soc.* **1987**, *109*, 5529–31. (c) Brown, T. L.; Butler, L. G.; Curtin, D. Y.; Hiyama, Y.; Paul, I. C.; Wilson, R. B. *J. Am. Chem. Soc.* **1982**, *104*, 1172–7. (d) Flygare, W. H. *J. Chem. Phys.* **1964**, *41*, 206–14. (e) Müller, C.; Idziak, S.; Pislewski, N.; Haeberlen, U. *J. Magn. Reson.* **1982**, *47*, 227–39. (f) Barfield, M.; Gottlieb, H. P. W.; Doddrell, B. M. *J. Chem. Phys.* **1978**, *69*, 4504–15.
(18) (a) Spiess, H. W. *NMR: Basic Princ. Prog.* **1978**, *15*, 59. (b) See ref 14 in this work and references therein.
(19) Olympia, P. L.; Wei, I. Y.; Fung, B. M. *J. Chem. Phys.* **1969**, *51*, 1610–4.

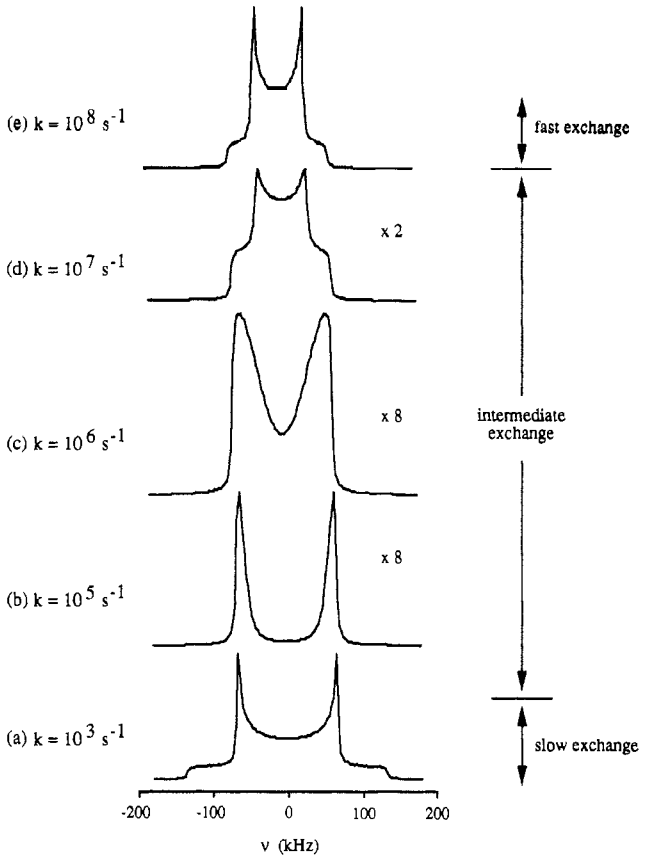

Figure 1. Calculated effect of the exchange rate on the deuterium NMR line shape for a cyclopentadienyl ring executing five-site nearest-neighbor jumps as shown in I: (a) slow-exchange regime; (b–d) intermediate-exchange regime; (e) fast-exchange regime. Spectra for the intermediate-exchange rates are vertically expanded by the factors shown in the figure.

transverse relaxation time, T_2, becomes comparable to the delay between pulses in the echo experiment, $t_1 = 30$ μs. T_2 is orientation-dependent, and, for those orientations or frequencies in the powder pattern for which T_2 is close to t_1, the last pulse in the quadrupole echo pulse sequence does not refocus the magnetization evolution due to the irreversible jump dynamics and there is a corresponding loss of spectral intensity.[3g,20] This is clearly seen in Figure 1b,c; when $k = 10^5$ s^{-1}, the intensity at frequencies around shoulders and between the peaks of the spectrum is reduced to nearly zero and is then regained at $k = 10^6$ s^{-1}. Thus, for motions occurring in the range 10^5–10^8 s^{-1}, the model and rate of motion can be determined by comparing the line shapes of simulated spectra to the fully relaxed experimental spectra acquired at different values of t_1.

For rates greater than 10^8 s^{-1}, the fast-exchange limit, the line shape of the deuterium powder pattern becomes independent of the rate of motion. As shown in Figure 1e, the typical powder pattern in the fast-exchange regime for a Cp ring executing five-site nearest-neighbor jumps is very similar to the static case (Figure 1a), except that the splitting between the peaks (and the corresponding splitting between the shoulders) is reduced and represents a motionally averaged value of the electric field gradient tensor. For Cp rings undergoing five-site nearest-neighbor jumps, the splitting corresponding to the motionally averaged electric field gradient tensor can be estimated from[21]

$$\overline{\Delta\nu} = \frac{\Delta\nu}{2}(3\cos^2\theta - 1) \qquad (2)$$

where θ is the angle formed by the C–^{2}H bonds and the C_5 rotation axis of the ring. On the basis of $e^2q_{zz}Q/h = 198$ kHz,

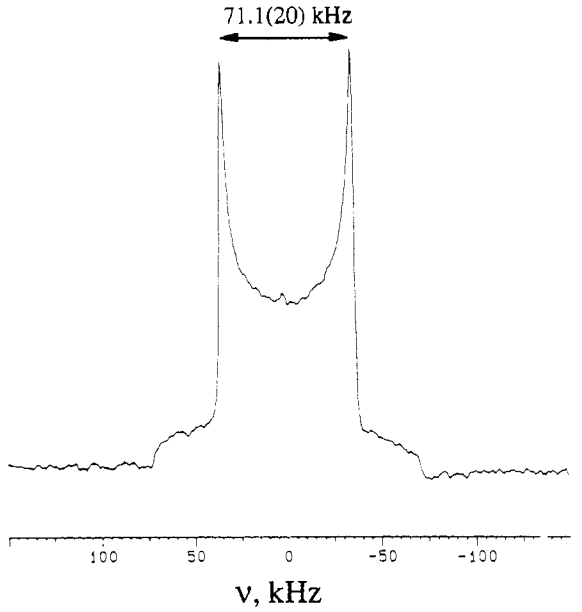

Figure 2. Experimental fully relaxed powder pattern for $(\mu\text{-CO})_2[\text{FeCp}^d(\text{CO})]_2$($Cp^d$ = ca. 70% deuteriated η^5-cyclopentadienyl). The line shape remains unchanged in the 100–300 K temperature range for the quadrupole echo pulse sequence with $t_1 = 30$ μs and $t_2 = 31$ μs.

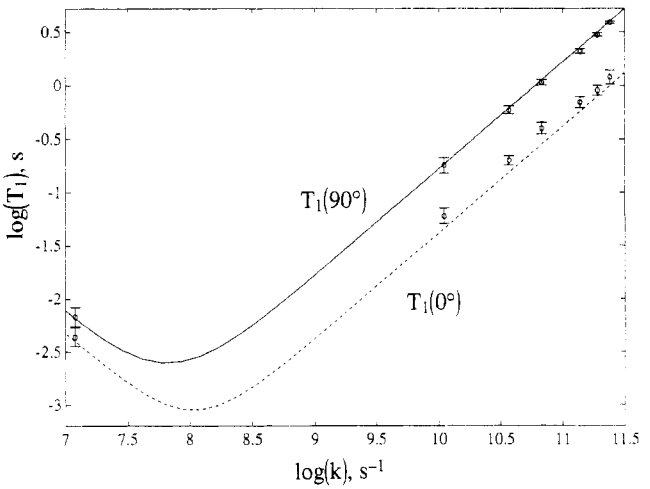

Figure 3. Plot of the experimental values of $T_1(90°)$ and $T_1(0°)$ versus log k, where k values are the rates of motion obtained from the simulated inversion–recovery spectra and listed in Table I. The traces are the theoretical T_1 values obtained from eqs 3–5.

fast exchange with θ = 90° should yield $\overline{\Delta\nu_1} = 74.2$ kHz. Figure 2 shows the experimental deuterium powder pattern taken at 300 K. The measured splitting is 71.1 (20) kHz. Thus the exchange rate for C_5 motion is greater than 10^8 s^{-1}, provided the mode of motion is indeed C_5 exchange.

Determination of Rates of Motion from the Anisotropy in T_1. In the fast-exchange limit, information on the dynamics is obtained from the deuterium spin–lattice relaxation times. Deuterium spin–lattice relaxation times are anisotropic in the solid state; in other words, the frequencies corresponding to different orientations of the C–^{2}H bond with the magnetic field have different T_1 values.[21] Torchia and Szabo have presented a methodology for constructing analytical expressions that describe deuterium spin–lattice relaxation times as a function of the jump rate for an N-site jump motion. Here, we give the expression for T_1 for a five-site jump, assuming $\eta = 0$:

$$\frac{1}{T_1} = \frac{3\pi^2}{4}\left(\frac{e^2qQ}{h}\right)^2[J_1(\omega_1) + 4J_2(2\omega_1)] \qquad (3)$$

where the spectral density functions are given by

(20) Spiess, H. W.; Sillescu, H. *J. Magn. Res.* **1981**, *42*, 381–9.
(21) Torchia, D. A.; Szabo, A. *J. Magn. Res.* **1982**, *49*, 107–21.

$$J_1(\omega_I) = \left\{\left[\frac{1}{2}(2\cos\theta - 1)(\cos\theta + 1)\right]^2 + \left[\frac{1}{2}(2\cos\theta + 1)(1 - \cos\theta)\right]^2\right\}(3\sin^2\Theta\cos^2\Theta) \times \frac{4k\sin^2\left(\frac{\pi}{5}\right)}{\left[4k\sin^2\left(\frac{\pi}{5}\right)\right]^2 + \omega_I^2} + \left[\frac{1}{4}(\sin^2\theta)(1 + \cos\theta)^2 + \frac{1}{4}(\sin^2\theta)(\cos\theta - 1)^2\right]\left(\frac{3}{4}\sin^4\Theta\right)\frac{4k\sin^2\left(\frac{2\pi}{5}\right)}{\left[4k\sin^2\left(\frac{2\pi}{5}\right)\right]^2 + \omega_I^2} \quad (4)$$

and

$$J_2(2\omega_I) = \left[\frac{1}{4}(\sin^2\theta)(1 + \cos\theta)^2 + \frac{1}{4}(\sin^2\theta)(\cos\theta - 1)^2\right] \times (3\sin^2\Theta\cos^2\Theta)\frac{4k\sin^2\left(\frac{\pi}{5}\right)}{\left[4k\sin^2\left(\frac{\pi}{5}\right)\right]^2 + 4\omega_I^2} + \left[\cos^8\left(\frac{\theta}{2}\right) + \sin^8\left(\frac{\theta}{2}\right)\right]\left(\frac{3}{4}\sin^4\Theta\right)\frac{4k\sin^2\left(\frac{2\pi}{5}\right)}{\left[4k\sin^2\left(\frac{2\pi}{5}\right)\right]^2 + 4\omega_I^2} \quad (5)$$

and where Θ is the angle between the rotation axis and the z axis of the static electric field gradient tensor (effectively, the C–^{2}H bond vector) as shown in I. The angle θ refers to the spectral frequencies for the parallel and perpendicular orientations of the C_5 rotation axis with respect to the magnetic field, similar to the static situation shown in II. The traces in Figure 3 are the theoretical $T_1(0°)$ and $T_1(90°)$ curves as a function of k, the jump rate. From Figure 3, it is clear that, for a five-site jump model with $\Theta = 90°$, T_1 is anisotropic for fast motions: $T_1(0°) \neq T_1(90°)$.

While it is possible to use the $T_1(0°)$ and $T_1(90°)$ experimental values and the theoretical spin–lattice relaxation times curves of Figure 3 to determine the jump rate, we have elected to determine jump rates by comparison of the partially relaxed deuterium powder patterns obtained from an inversion–recovery experiment with the spectral simulations obtained from the computer program SPOWDER. We want to emphasize that, with the dual methods of (1) comparing simulated and experimental partially relaxed spectra and (2) fitting the experimental T_1 values to the theoretical T_1 curves, one does not gain further information about the model of motion. However, the former method gives information on the angular dependence of T_1 for all the possible values of the angle θ when the whole set of partially relaxed powder patterns is analyzed; this permits one to obtain a more accurate value for the jump rate and the corresponding error limit (vide infra).

Results

T_1 experiments were done for $(\mu\text{-CO})_2[FeCp^d(CO)]_2$ for seven different temperatures in the range 100–300 K. Figures 4 and 5 show the experimental data and the corresponding best matching set of simulated inversion–recovery spectra at 209 K. In order to decide which rate produced the best set of simulated spectra and to estimate the error limits for the reported rate constant, the simulated and the experimental powder patterns of the partially relaxed spectra around the inversion point were carefully compared. Figure 6 shows how the effect of changing the rate is easily observed around the inversion point; when $k = 3.7 \times 10^{10}$ s^{-1}, a good match is obtained between the simulated and experimental (compare to Figure 4), but for rates equal to 2.5×10^{10} and 4.9×10^{10} s^{-1}, the relaxation patterns are clearly too fast and too slow, respectively. For each of the seven temperatures, at least three sets of simulated spectra were used to determine the rates and to define the error limits as described above. The results are summarized in Table I.

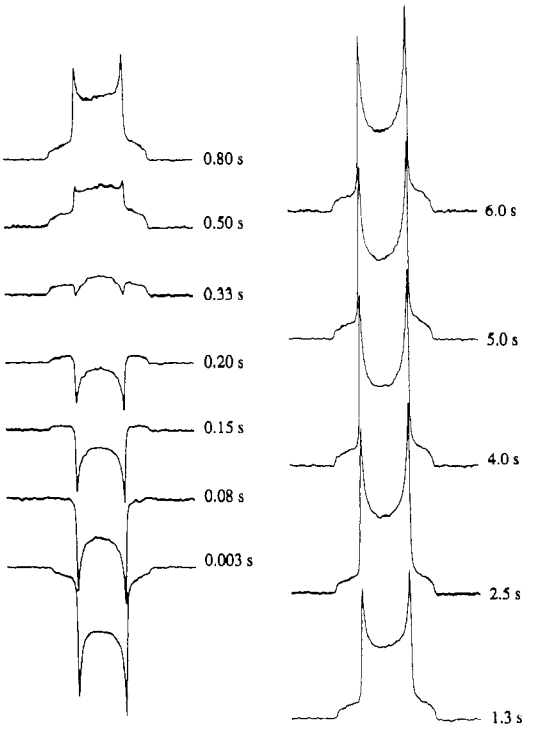

Figure 4. Experimental inversion–recovery spectra for $(\mu\text{-CO})_2[FeCp^d(CO)]_2$ obtained at 209 K. The variable delays, τ, are shown beside each spectrum.

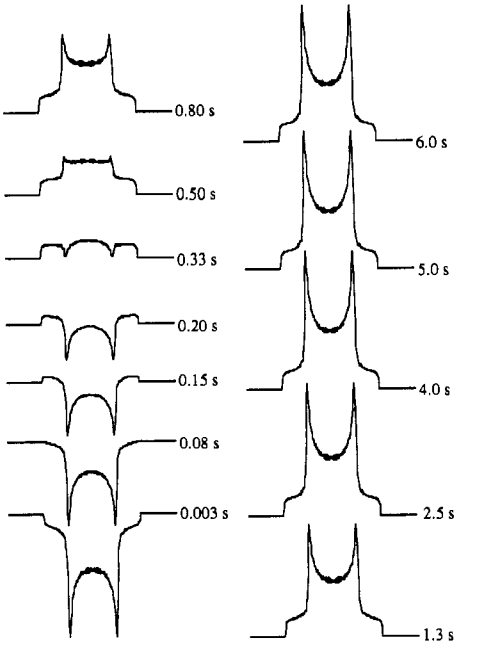

Figure 5. Simulated inversion–recovery spectra for $(\mu\text{-CO})_2[FeCp^d(CO)]_2$ for $k = 3.7 \times 10^{10}$ s^{-1}. The variable delays, τ, are shown beside each spectrum.

A plot of the experimental values of $T_1(90°)$ and $T_1(0°)$ versus log k is shown in Figure 3; k in this case is the jump rate as obtained from the spectral simulations of the inversion–recovery data and listed in Table I. The traces are the theoretical T_1 values obtained from eqs 3–5. Even though the excellent match for both $T_1(90°)$ and $T_1(0°)$ seems to confirm that the five-site nearest-neighbor jump is a simple suitable model for the reorientation of the Cp ring, it should be pointed out that there is a distinct possibility that next-nearest-neighbor jumps, C_5^2 rotations, occur in addition to nearest-neighbor jumps, C_5 rotations. Since the slopes of the T_1 curves for $T_1(90°)$ and $T_1(0°)$ for the two models, C_5 and C_5^2 rotations, are the same, the T_1 anisotropy cannot be

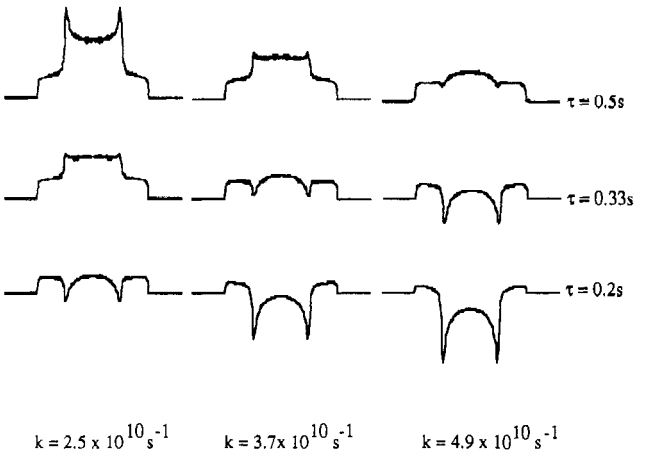

Figure 6. Effect of the jump rate on the primarily relaxed spectra about the inversion point in the inversion–recovery experiment. The simulated spectra are for comparison with inversion–recovery spectra obtained at 209 K. The selected variable delays, τ, are indicated at the right of each row, and the jump rates are below each column.

Table I. Summary of the Results Obtained from the Analysis of the Experimental and Simulated Inversion–Recovery Spectra for $(\mu\text{-CO})_2[\text{FeCp}^d(\text{CO})]_2$

T, K	k, s^{-1} [a]	$T_1(90°)$, s	$T_1(0°)$, s
100	1.20 (24) × 10^7	0.0068 (14)	0.0044 (9)
178	1.10 (20) × 10^{10}	0.18 (3)	0.06 (1)
209	3.7 (7) × 10^{10}	0.59 (5)	0.20 (2)
229	6.8 (12) × 10^{10}	1.07 (6)	0.40 (5)
260	1.38 (28) × 10^{11}	2.10 (10)	0.70 (8)
280	1.9 (4) × 10^{11}	3.00 (10)	0.90 (10)
300	2.4 (5) × 10^{11}	3.91 (10)	1.20 (18)

[a] Defined as jump rate between nearest-neighbor sites. Uncertainty in parentheses. Note: An alternative convention used in solution NMR chemical exchange differs by a factor of 2π, k(chemical exchange) = k(table)/2π.[25]

used to distinguish between the two models. Fortunately, the two models have different T_2 anisotropies in the intermediate-exchange regime. Thus, from a line-shape analysis of the fully relaxed deuterium powder patterns acquired by varying t_1 in the quadrupole echo pulse sequence, the C_5 and C_5^2 rotational modes can be distinguished. In order to analyze the T_2 anistropy, fully relaxed deuterium powder patterns were obtained with four different values of t_1 (30, 60, 120, and 240 μs) at 100 K, where the rate of motion, 1.2 × 10^7 s^{-1}, falls in the intermediate-exchange regime. As shown in Figure 7 for a t_1 of 120 μs, the experimental spectrum (Figure 7a) matches the simulated powder pattern for C_5 rotations (Figure 7b) better than that for C_5^2 rotations (Figure 7c). Thus, on the basis of T_2 anisotropy, the predominant mode of motion in the 100 K range is the nearest-neighbor jump model. These results agree with the results obtained by solid-state ^{13}C NMR spectroscopy for the rotation of the permethylcyclopentadienyl ligand, Cp*.[22] In that work, a line-shape analysis of the solid-state ^{13}C NMR powder pattern of the Cp* ligand in $(Cp^*)_2Fe$ showed that the nearest-neighbor jump model was also strongly favored over the next-nearest-neighbor jump model at 101 K.

From the rates obtained at different temperatures, we are able to estimate kinetic parameters for the C_5 rotation for the cyclopentadienyl ring. In Figure 8, rates and temperatures are plotted according to the Arrhenius equation. The line has a slope and intercept that yield an activation energy, E_a, and preexponential factor of 12.5 (3) kJ/mol and 4.4 (8) × 10^{13} s^{-1}, respectively.

Discussion

The activation energy of 12.5 (3) kJ/mol falls within the range of values found from other techniques for the reorientation of the Cp ring in organometallic compounds. This value for the activation energy is higher than the values of 7.24 and 7.15 kJ/mol obtained for the monomers $Cp(CO)_3Mn$ and $Cp(CO)_3Re$, respectively, but similar to the value of 13.06 kJ/mol obtained for the dimer $[Mo(CO)_3Cp]_2$; these rate processes were studied in the solid state via proton NMR spin–lattice relaxation times.[7]

For the monomers $Cp(CO)_3M$ (M = Re, Mn), the origin of the barrier of rotation is assigned to intermolecular interactions on the basis of two observations: First, the change in electronic energy associated with the rotation of the Cp ring in these com-

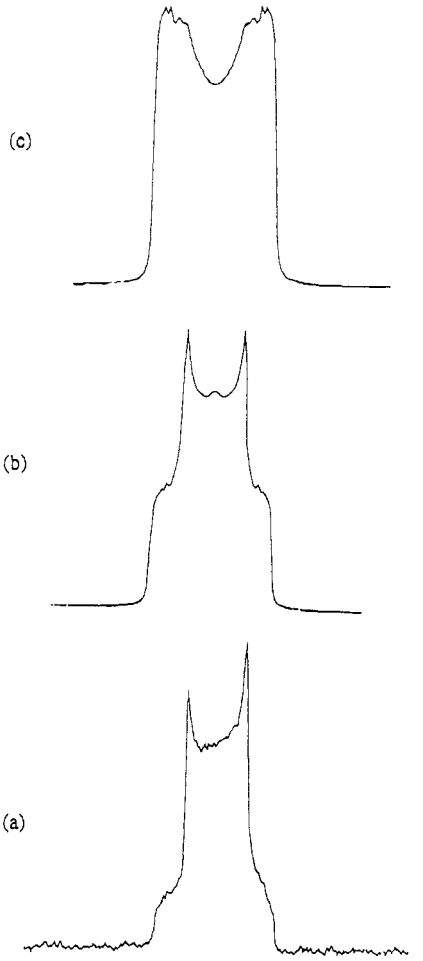

Figure 7. Experimental and simulated spectra showing the T_2 anisotropy for t_1 = 120 μs and t_2 = 121 μs: (a) experimental spectrum obtained at 100 K; (b) simulated spectrum for C_5 rotations with k = 1.2 × 10^7 s^{-1}; (c) simulated spectrum for C_5^2 rotations with k = 1.2 × 10^7 s^{-1}.

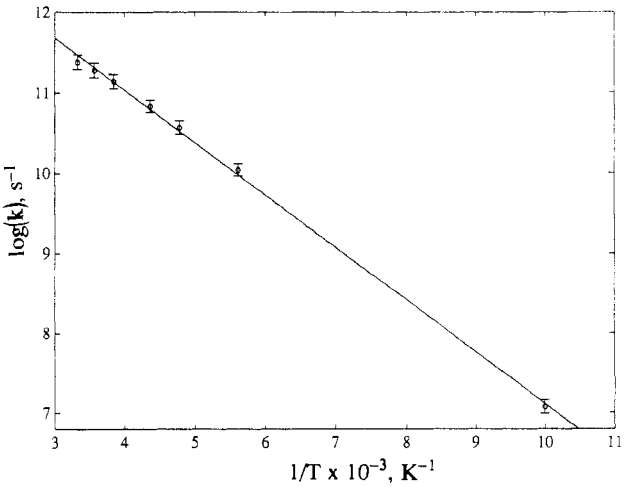

Figure 8. Arrhenius plot for the cyclopentadienyl ring rotation in $(\mu\text{-CO})_2[\text{FeCp}^d(\text{CO})]_2$. The errors are represented by the vertical bars, and the solid line is the best least-squares fit with uniform (average) weights to the data listed in Table I.

(22) Wemmer, D. E.; Ruben, D. J.; Pines, A. *J. Am. Chem. Soc.* **1981**, *103*, 28–33.

plexes is predicted to be 8.4×10^{-3} kJ/mol on the basis of molecular orbital calculations;[23] this is about 3 orders of magnitude smaller than the observed activation energy. Second, a comparison of the experimental values of the activation energies with the predicted values based on the nonbonded atom-atom interaction indicates that the potential energy surface for Cp ring reorientation is dominated by the intermolecular interactions of the types Cp-Cp and Cp-CO.[7a] Moreover, intermolecular forces also seem to play an important role in the activation energy for the Cp ring rotation in ferrocene; the activation energy for Cp ring rotation in ferrocene in 4 kJ/mol in the gas phase as measured from electron diffraction studies[24] whereas, in the solid state, the barrier is 8.3 kJ/mol as measured from proton NMR spin-lattice relaxation times.[7c] Since the activation energy found for $(\mu\text{-CO})_2[\text{FeCp(CO)}]_2$ is 12.5 (3) kJ/mol, it is likely that the rotation barrier originates with the contacts between nonbonding atoms rather than from electronic factors. The fact that both $(\mu\text{-CO})_2[\text{FeCp(CO)}]_2$ and $[\text{Mo(CO)}_3\text{Cp}]_2$ have higher Cp ring rotation barriers than those of $\text{Cp(CO)}_3\text{Mn}$ and $\text{Cp(CO)}_3\text{Re}$ may be due to the effect of intramolecular contacts present in the dimers (i.e., half of the molecule interacting with the other half) but not in the monomers.

Conclusions

We have determined the characteristics of the cyclopentadienyl ring rotation in $(\mu\text{-CO})_2[\text{FeCp(CO)}]_2$ in the solid state by analysis of the anisotropy of the deuterium spin-lattice relaxation times in the temperature range 100-300 K. Our results show that the reorientation of the Cp ligands in the solid state proceeds with nearest-neighbor jump rates in the range 1.20 (24) $\times 10^7$ to 2.4 (5) $\times 10^{11}$ s^{-1}. The activation energy for the ring rotation has been estimated to be 12.5 (3) kJ/mol. On the basis of T_2 anisotropy experiments, C_5 rotations rather than C_5^2 rotations are dominant at 100 K, and since the Arrhenius plot is linear in the range 100-300 K, C_5 rotations seem to prevail for all temperatures studied.

One conclusion of this work is that there is a good agreement between our results and the results obtained from Raman spectroscopy, from quasi-elastic neutron scattering, and especially from proton NMR spin-lattice relaxation times for Cp ring rotation in other complexes. This shows that solid-state deuterium NMR spectroscopy is an excellent alternative for the study of solid-state motions in organometallic compounds. More importantly, deuterium NMR methods have the special advantage of selective labeling, thus overcoming the frequent problem of assignment of the spectral lines in the Raman or quasi-elastic neutron scattering experiments. Another advantage of using solid-state deuterium NMR spectroscopy for motional studies is that both the model of motion and the rate of motion can be evaluated simultaneously; in all the other techniques, except for quasi-elastic neutron scattering, the data directly available from the experiment are the kinetic parameters, but little is learned directly about the type of motion associated with those parameters, as assumptions must be made about the mode of motion.

Acknowledgment. The support of the National Science Foundation (Grant CHE8715517), the donors of the Petroleum Research Fund, administered by the American Chemical Society, and the LSU Center for Energy Studies is gratefully acknowledged (L.G.B.). The purchase of the solid-state 200-MHz NMR spectrometer (LSU) was made possible by NSF Grant CHE8711788.

(23) (a) Albright, T. A.; Hoffmann, P.; Hoffmann, R. *J. Am. Chem. Soc.* **1977**, *99*, 7546-57. (b) Albright, T. A.; Hoffmann, R.; Tse, Y.; D'Ottavio, T. *J. Am. Chem. Soc.* **1979**, *101*, 3812-21.
(24) Haaland, A.; Nilsson, J. E. *Acta Chem. Scand.* **1968**, *22*, 2653-70.
(25) Carrington, A.; McLachlan, A. D. *Introduction to Magnetic Resonance*; Harper and Row: New York, 1967.

Contribution from the Institut Laue-Langevin, 156X, 38042 Grenoble Cedex, France, and Department of Chemistry, University of Toronto, Toronto, Ontario M5S 1A1, Canada

Dynamics of Molecular Hydrogen in the Complex *trans*-$[\text{Fe}(\eta^2\text{-H}_2)(\text{H})(\text{PPh}_2\text{CH}_2\text{CH}_2\text{PPh}_2)_2]\text{BF}_4$ in the Solid State As Revealed by Neutron-Scattering Experiments

Juergen Eckert,*[†,‡] Herma Blank,[†] Maria T. Bautista,[§] and Robert H. Morris[§]

Received July 5, 1989

The vibrational spectrum of the $\text{Fe}(\eta^2\text{-H}_2)\text{H}$ fragment in *trans*-$[\text{FeH}(\text{H}_2)(\text{PPh}_2\text{CH}_2\text{CH}_2\text{PPh}_2)_2]\text{BF}_4$ has been obtained by inelastic neutron scattering in the range 200-1000 cm^{-1}. High-resolution neutron spectroscopy was also utilized to observe the rotational tunnel splitting of the librational ground state of the dihydrogen ligand at 2.1 cm^{-1}. This and the torsional transitions assigned at 225 and 255 cm^{-1} are consistent with a modulated double-minimum potential for rotation with one angular degree of freedom. The resulting barrier to rotation of about 2.3 kcal/mol is discussed in terms of its origin in electronic and steric factors and compared with similar results on other molecular hydrogen complexes.

Most of the dynamical information on the $\eta^2\text{-H}_2$ ligand in the recently discovered[1] molecular hydrogen complexes has been obtained from NMR measurements.[2-5] In fact, in a vast majority of these compounds NMR evidence is the primary indicator for the presence of the dihydrogen ligand. These measurements typically show values for δ of -3 to -12 in the ^{1}H NMR spectrum and in the isotopically substituted complexes show large values of J(H,D) that are well above those for hydride-deuteride coupling but below that for HD in the gas phase. In addition, the minimum value of T_1 can also be taken as a diagnostic for the presence of the $\eta^2\text{-H}_2$ ligand, and such data can in fact be analyzed to yield H-H separations under the assumption that dipolar relaxation dominates T_1.[3,4] NMR measurements have also been successful at monitoring the exchange between dihydrogen and hydride ligands in cases where the latter is present.[6-15] Vibrational data

† Institute Laue-Langevin.
‡ Permanent address: LANSCE, Mail Stop H805, Los Alamos National Laboratory, Los Alamos, NM 87545.
§ University of Toronto.

(1) Kubas, G. J. *Acc. Chem. Res.* **1988**, *21*, 120.
(2) Kubas, G. J.; Unkefer, C. J.; Swanson, B. I.; Fukushima, E. *J. Am. Chem. Soc.* **1986**, *108*, 7000.
(3) Bautista, M. T.; Earl, K. A.; Maltby, P. A.; Morris, R. H.; Schweitzer, C. T.; Sella, A. *J. Am. Chem. Soc.* **1988**, *110*, 7031.
(4) Hamilton, D. G.; Crabtree, R. H. *J. Am. Chem. Soc.* **1988**, *110*, 4126.
(5) Zilm, K. W.; Merrill, R. A.; Kummer, M. W.; Kubas, G. J. *J. Am. Chem. Soc.* **1986**, *108*, 7837.
(6) Crabtree, R. H.; Lavin, M.; Bonnevoit, L. *J. Am. Chem. Soc.* **1986**, *108*, 4032.
(7) Bautista, M. T.; Earl, K. A.; Maltby, P. A.; Morris, R. H. *J. Am. Chem. Soc.* **1988**, *110*, 4056.
(8) Bautista, M.; Earl, K. A.; Morris, R. H.; Sella, A. *J. Am. Chem. Soc.* **1987**, *109*, 3780.

0020-1669/90/1329-0747$02.50/0